Proceedings of the 6th International Conference on Gas Hydrates (ICGH 2008), Vancouver, British Columbia, CANADA, July 6-10, 2008.

RAMAN STUDIES OF METHANE-ETHANE HYDRATE STRUCTURAL TRANSITION

Hiroshi Ohno, Timothy A. Strobel, Steven F. Dec, E. Dendy Sloan, and Carolyn A. Koh *
Center for Hydrate Research
Colorado School of Mines
Golden, Colorado 80401
USA

ABSTRACT

The inter-conversion of methane-ethane hydrate from metastable to stable structures was studied using Raman spectroscopy. To investigate factors controlling the inter-conversion, the rate of structural transition was measured at 59% and 93% methane in ethane. The observed slower structural conversion rate in the lower methane concentration atmosphere can be explained in terms of the differences in kinetics (mass transfer of gas and water rearrangement). Also, the effect of kinetic hydrate inhibitors, poly-N-vinylpyrrolidone (PVP) and polyethylene-oxide (PEO), on the hydrate metastability was investigated at 65% and 93% methane in ethane. PVP increased the conversion rate at 65% methane in ethane (sI is thermodynamically stable), but retarded the rate at 93% methane in ethane (sII is thermodynamically stable), indicating that the function of PVP depends on hydrate structure. PEO did not affect the structural transition considerably for either methane-ethane compositions.

Keywords: natural gases, gas hydrates, kinetic inhibitors

INTRODUCTION

Gas hydrates (also called clathrate hydrates) are generally formed at low temperatures and high pressures, and are comprised of water cage structures which enclathrate guest gases of the appropriate size and shape [1]. Natural gas hydrate formation can cause blockages in subsea gas and oil flow lines, which can lead to catastrophic economic and safety concerns [2]. Therefore, the prevention and removal of gas hydrates during natural gas and oil subsea production and transportation are major concerns of the energy industries [3-5].

Most gas hydrates crystallize into one of the two cubic systems, structure I (sI) or structure II (sII) [1]. A unit cell of sI consists of 46 water molecules that form two pentagonal dodecahedral cavities with twelve pentagonal faces (5^{12}) and six tetrakaidecahedral cavities with twelve pentagonal faces and two hexagonal faces ($5^{12}6^2$). A unit cell of sII comprises 136 water molecules that form sixteen 5^{12} cages and eight hexakaidecahedral cavities with twelve pentagonal faces and four hexagonal faces ($5^{12}6^4$).

The two main constituents of natural gases are methane and ethane, which account for more than 93% of the average gas composition [1]. Pure methane and pure ethane each form sI hydrate. sI hydrate is also formed from methane-ethane mixtures containing approximately up to 75% methane and above 99% methane. Conversely, sII hydrate is formed from methane-ethane mixtures containing approximately between 75−99% CH_4 [6]. This interesting phenomenon was predicted theoretically by Hendriks et al. [7] and later confirmed by Subramanian et al. [8, 9] using NMR and Raman spectroscopy. The sI to sII transition can be explained by considering the relative stabilities of methane and ethane in the cages of the two hydrate structures, along with the ratio of

* Corresponding author: Phone: +1 303 273 3237 Fax +1 303 273 3730 E-mail: ckoh@mines.edu

large to small cavities present in each unit cell. At high ethane concentrations, sI is the thermodynamically favored phase as ethane preferentially occupies the larger $5^{12}6^2$ cavities, rich in sI (a ratio of 3:1 = $5^{12}6^2$:5^{12}). As the composition of methane is increased, the transition to sII occurs due to the abundance of methane and the large number of small cavities (a ratio of 2:1 = 5^{12}:$5^{12}6^4$) in sII. This trend causes sII to be the incipient hydrate phase for progressively higher concentrations of methane, until, very high (99^+%) concentrations of methane are present (see refs. [10, 11] for more details). At gas compositions close to the sI/sII transition points, the two structures coexist as a metastable state [9, 12, 13].

Recently, we investigated the degree of metastability of methane-ethane hydrates formed from gas mixtures of 65% or 93% methane in ethane and water using Raman spectroscopy [14].

A main finding of this study was that the rate of inter-conversion from metastable to stable structures in the higher methane concentration atmosphere was much faster. We propose two possible causes for this observation: (1) the differences in the driving force and (2) kinetics of the inter-conversion, namely, the difference in the chemical potential of water in sI compared to sII, and the degree of guest-gas redistribution and the activation energy for water rearrangement.

Also, it was found that the presence of poly-N-vinylcaprolactam (PVCap; an effective kinetic hydrate inhibitor [15]) affects the metastability, at 65% CH_4 the inhibited system contained less metastable sII than the pure system, while at 93% CH_4 the conversion rate was two orders of magnitude slower than the pure system.

Understanding the nature of the methane-ethane hydrate metastability is an important problem for the gas and oil industry because the formation of a sI and sII mixture and subsequent inter-conversion from a metastable to a stable structure are likely to occur in pipelines. Essential information for the pipeline flow assurance industry, such as dissociation pressure (or temperature) and heat capacity of the hydrate, are strongly dependent on crystal structure [1]. As another example of industrial importance, if a kinetic hydrate inhibitor is designed for sII inhibition, but sI is the predominant, metastable, hydrate former, then the inhibitor may prove ineffective. However, there have been few studies reported that have investigated the above phenomena quantitatively.

In this work, we quantify the degree of the methane-ethane hydrate metastability at two gas compositions of 59 mole% and 93 mole% methane in ethane as a function of time using Raman spectroscopy. The rate-determining factors of the inter-conversion have been investigated. The influence of two kinetic hydrate inhibitors with different performance, poly-N-vinylpyrrolidone (PVP; moderate hydrate inhibitor) and poly-ethylene-oxide (PEO; poor hydrate inhibitor), was also investigated.

EXPERIMENTAL METHODS

Hydrate samples

Methane-ethane hydrates were synthesized in a high-pressure cell with 1 cm^3 capacity and a sapphire window of diameter 1.5 cm (Figure 1; manufactured by Sam O. Colgate, Inc.).

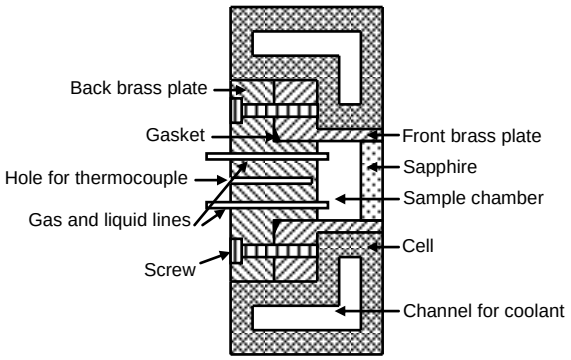

Figure 1: Schematic of the high-pressure Raman cell

The evacuated cell was half-filled with de-ionized water without and with 0.008 wt.% PVP (ISP Technologies Inc) or PEO (Sigma-Aldrich). The filled cell was then charged with the methane-ethane gas mixture. For the discussion of rate-determining factors of the inter-conversion, pure hydrates were formed from two gas mixtures of 93 mole% methane (C1) at 8.4 MPa or 59 mole% C1 at 4.7 MPa.

The effect of the kinetic hydrate inhibitors were tested at two conditions of 93 mole% C1 at 8.4 MPa or 65 mole% C1 at 5.3 MPa. The gas mixtures were prepared by mixing pure methane (Matheson Tri Gas) and ethane (Airgas) gases gravimetrically. Fresh samples were prepared for each experiment.

The system temperature was then cooled from 20 ºC to inside the hydrate stable region at 1 ºC at a cooling rate of 0.3 ºC/min by circulating liquid coolant through a metal jacket surrounding the

cell. The sample was maintained at this constant temperature for the remainder of the experiment. The temperature was monitored using a thermocouple placed in a hole in the brass wall of the cell. At the three gas-composition and pressure conditions used, hydrate dissociation temperatures were 15 ºC. Therefore, the sub-cooling applied to the samples was 14 ºC for all cases.

The sample system was allowed to stand without agitation during the measurements. Since gas consumption due to hydrate formation was small, significant pressure drops and gas composition changes were not observed during the experiments.

Raman measurements

Raman spectra of the samples were obtained using a Renishaw MK III spectrometer equipped with a 2400 gr/mm grating and a multi-channel CCD detector [16, 17]. The laser source (wavelength of 514.5 nm) was focused to a diameter of approximately 5 μm onto the gas-hydrate (or gas-water) interface using a long-working-distance objective lens (Olympus SPlan 20×). At the interface the gas phase Raman signals suddenly decreased in intensity with vertical distance, and hydrate or water Raman signals appear when the laser focal point is below the gas phase.

Backscattered light was corrected with the objective lens and was sent to the spectrometer through an optical fiber system. Raman frequencies were calibrated using neon emission lines. Because the distribution of the hydrate structure was found to be spatially non-uniform, the laser focal point was changed for each measurement to obtain the overall structural feature of a sample. The data acquisition time for one measurement was from 30 to 180 seconds, depending on the intensity of the Raman scattering. Initially, hydrate structures were monitored for 6 hours after the first hydrate crystals were observed. When a hydrate sample had not reached its equilibrium structure within the 6 hour measurement period, further long-term observations of up to one week were performed. Approximately 100 independent Raman measurements were performed on a given sample.

Reference spectra

Figure 2 shows Raman spectra of the methane-ethane gas mixtures and hydrates, which were obtained as reference data. The hydrates were synthesized from the gas mixtures and de-ionized water using the procedure described above. To eliminate signals from the gas phase, hydrate phase positions approximately 1 mm below the gas-hydrate (or gas-water) interfaces were measured.

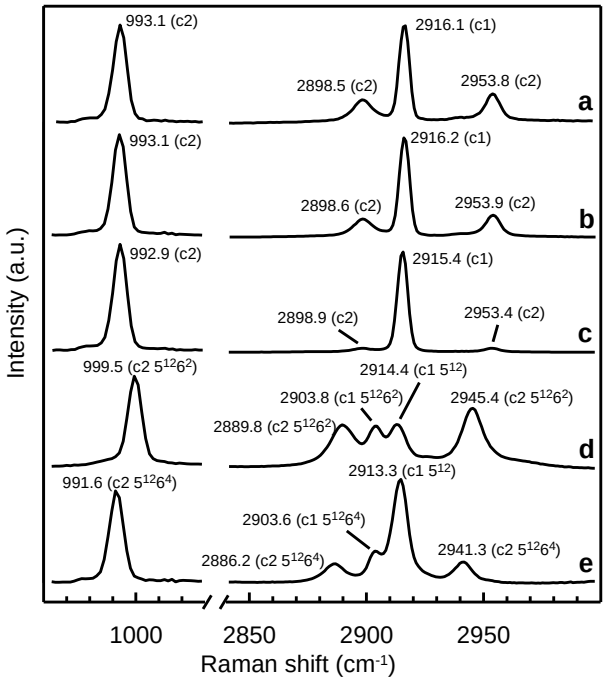

Figure 2: Raman spectra of the C-C stretching mode (~1000 cm^{-1}) and C-H stretching mode (~2900 cm^{-1}) regions at 1 ºC. (a) Methane-ethane gas mixture of 59% CH_4 at 4.7 MPa. (b) Methane-ethane gas mixture of 65% CH_4 at 5.3 MPa. (c) Methane-ethane gas mixture of 93% CH_4 at 8.4 MPa. (d) Methane-ethane structure I hydrate formed from the gas-mixture **b**. (e) Methane-ethane structure II hydrate formed from the gas-mixture **c**. The hydrate spectra were recorded about one week after the crystal nucleation. The peak assignments are based on Subramanian et al.[8, 9].

The hydrate spectra were recorded about one week after the hydrate nucleation had been completed. Gas phase methane (Figure 2a, b and c) has a C-H stretching mode at around 2915 cm^{-1} [8, 9]. Gas phase ethane (Figure 2a, b and c) has a C-H stretching mode which splits into two bands due to coupling with one of the CH_3 deformation modes at approximately 2899 and 2953 cm^{-1} and a C-C stretching mode at approximately 993 cm^{-1} [8, 9]. These bands shift and split when the gas molecules are enclathrated by the host water molecules (Figure 1d and e) [8, 9, 18].

The statistical thermodynamics program CSMGem [19] predicts that structure I hydrate is stable in the 65 mole% CH_4 sample, while structure II hydrate

is stabilized in the 93 mole% CH_4 sample. As predicted, the hydrate spectrum of the 65% CH_4 sample (Figure 2d) and that of the 93% CH_4 sample (Figure 2e) agree well with the previously reported Raman spectra of methane-ethane structure I hydrate and that of methane-ethane structure II hydrate, respectively [8, 9]. Peak assignments for the sI and sII methane-ethane hydrates based on our previous work [8, 9] are shown in Figure 2.

Spectra analysis

The hydrate structures of the samples were determined by analyzing the higher-frequency ethane C-H band. This band is optimum for peak-fitting analysis because the Raman frequencies of this band differ by several cm^{-1} between the gas phase and the two hydrate structures. Also, this mode does not overlap with other bands in the spectra (Figure 2). Figure 3 shows examples of spectra recorded in this study and the results of the peak-fitting analyses. Deconvolution of the peaks was performed using a commercial peak fitting program (GRAMS/AI, Galactic Industries). Peak fitting parameters of the ethane band were obtained from the reference spectra (Figure 2 and Table 1).

These parameters were constrained for all subsequent spectral deconvolutions. Hydrate structural composition can be related to the Raman peak area contribution of C_2H_6 in the $5^{12}6^4$ cavities, $I_{C2,5^{12}6^4}$, and that in $5^{12}6^2$ cavities, $I_{C2,5^{12}6^2}$, according to equation (1). This includes the assumption that the scattering cross section of C_2H_6 molecules is independent of the type of surrounding water cage:

$$V_{h,sII} = \frac{\left(\frac{I_{C2,5^{12}6^4}}{N_{5^{12}6^4}\theta_{5^{12}6^4,C2}} \right)}{\left(\frac{I_{C2,5^{12}6^2}}{N_{5^{12}6^2}\theta_{5^{12}6^2,C2}} + \frac{I_{C2,5^{12}6^4}}{N_{5^{12}6^4}\theta_{5^{12}6^4,C2}} \right)} \qquad (1)$$

where $V_{h,sII}$ is the volume fraction of structure II hydrate in the hydrate phase; $N_{5^{12}6^2}$ and $\theta_{5^{12}6^2,C2}$ are the number concentration and ethane occupancy of $5^{12}6^2$ cavities in sI hydrate while $N_{5^{12}6^4}$ and $\theta_{5^{12}6^4,C2}$ are those of $5^{12}6^4$ cavities in sII hydrate, respectively. $N_{5^{12}6^2}$ and $N_{5^{12}6^4}$ values calculated from crystal structures [1] are 3.47 and 1.55 nm^{-3}, respectively. The CSMGem program [19] was used to estimate that $\theta_{5^{12}6^2,C2}$ and $\theta_{5^{12}6^4,C2}$ values of 0.82 and 0.96 in the 59% CH_4 sample, 0.77 and 0.94 in the 65% CH_4 sample, and 0.28 and 0.69 in the 93% CH_4 sample, respectively. By using Equation 1, the N_i and θ_l values, and the results of the peak fitting analyses, the hydrate structural composition was then calculated.

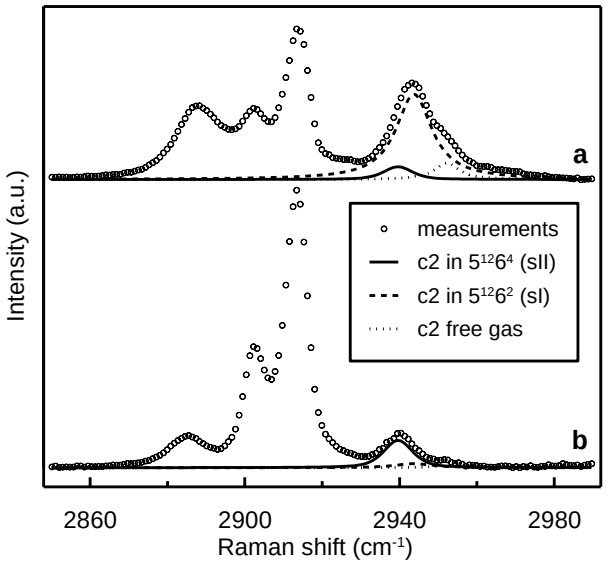

Figure 3: Raman spectra of methane-ethane hydrate in the vicinity of the gas/hydrate interface, and results of peak-fitting analysis for the higher frequency C_2H_6 C-H stretching mode. (a) 65% CH_4 at 1 ºC 5.3 MPa without KHI, 108 minutes after the first crystal was observed. (b) 93% CH_4 at 1 ºC 8.4 MPa without KHI, 82 minutes after the first crystal was observed.

	Peak-center (cm^{-1})	Half-width (cm^{-1})	Lorentz (%)
In 59% CH_4 gas at 4.7 MPa	2953.8	8.2	99
In 65% CH_4 gas at 5.3 MPa	2953.9	7.5	96
In 93% CH_4 gas at 8.4 MPa	2953.4	8.0	99
In $5^{12}6^2$ hydrate cage (sI)	2945.4	11.2	100
In $5^{12}6^4$ hydrate cage (sII)	2941.3	8.8	53

Table 1: Gaussian + Lorentzian peak parameters of the higher-frequency C-H band of C_2H_6 in methane-ethane gas mixtures or hydrate cages, obtained from the reference spectra (Figure 1).

RESULTS

Induction time

Results of the induction times for hydrate formation, i.e. the time to form the first hydrates as spectroscopically observed after the temperature drop, are tabulated in Table 2. Although there was a considerable difference in the induction time between the samples, more repeat measurements are needed to discuss the effect of the kinetic hydrate inhibitors or gas compositions on hydrate

nucleation due to the stochastic nature of this phenomenon.

	Induction time (min)
59% C1	91
65% C1 with PVP	90
65% C1 with PEO	193
93% C1 with PVP	101
93% C1 with PEO	71

Table 2: The induction time for hydrate formation.

Hydrate structure in pure samples at 59% C1

As discussed in this section, Raman analyses show the inter-conversion of methane-ethane hydrate from metastable to stable structures at 59% methane in ethane was much slower compared with the result at 93% methane in ethane.

Figure 4a and b represents the methane-ethane hydrate structural compositions of the 59% CH_4 samples versus time after the first hydrates were observed. Approximately 100 independent Raman measurements were performed on a given sample. In these experiments, structure I hydrate is the thermodynamically stable state (calculated from CSMGem [19]). The formation of sI + sII hydrate mixtures with approximately 29% sII were observed (Figure 4a). Although the hydrate structure observed with Raman spectroscopy was dependent on the focal point of the laser used, there was no systematic change in the structure with time during the 6 hour observation period (Figure 4a).

These results suggest that the spatial distribution of the hydrate structure was not uniform, but the average composition remained almost unchanged during the 6 hour time period. In the longer time period observation (several days; Figure 4b), the average volume fraction of sI crystals in the hydrate phase was observed to increase with the elapse of time, although the considerable amount of metastable sII still remained 2 days after the nucleation, indicating gradual hydrate structural transition.

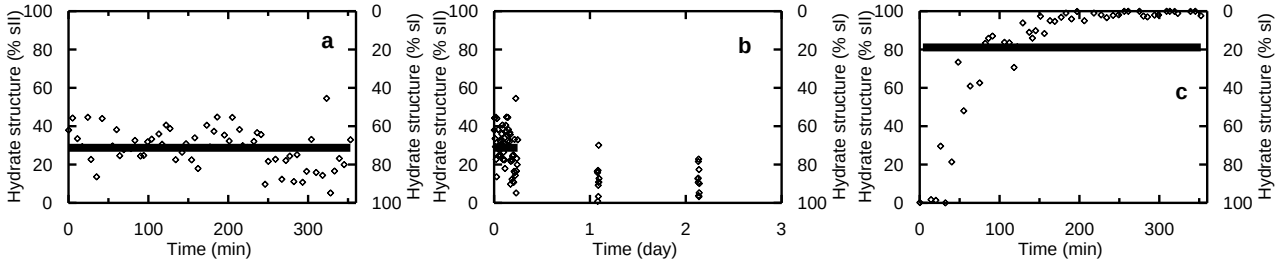

Figure 4: Methane-ethane hydrate structures in pure systems at 1 ºC in the vicinity of the gas/hydrate interfaces vs. time after the first crystals were observed. (a) and (b) Pure sample formed from 59% CH_4 at 4.7 MPa. (c) Pure sample formed from 93% C1 at 8.4 MPa. Solid symbols represent the mean values of duration of observation.

In contrast, we found in a previous study that the transition from metastable sI to stable sII completed only within a few hours in the 93% CH_4 sample [14]. In this 93% C1 system, hydrates initially observed were almost pure structure I crystals (Figure 4c). However, the fraction of sI hydrate rapidly decreased with time and was completely replaced by sII hydrate after approximately 3 hours, indicating a fairly rapid inter-conversion compared with the 59% CH_4 sample (days).

Hydrate structure in 65% and 93% C1 samples with PVP and PEO

There was a considerable difference in the hydrate inter-conversion rate between the samples with different types of kinetic hydrate inhibitors and also between the samples with different gas compositions.

Figure 5 represents the hydrate structural compositions of the 65% CH_4 samples measured as a function of time. For these samples, the predicted stable hydrate structure was sI (calculated using CSMGem [19]). For comparison with the new results of this study (Figure 5e-h), the results of pure and PVCap samples found in the previous study are shown in Figure 5a-d.

As discussed previously it took approximately one week to complete the inter conversion in the pure sample (Figure 5a and b), while metastable sII hydrate crystals were almost gone within a few days in the system with PVCap (Figure 5c and d), indicating that PVCap promotes the structural transition.

In the system with PVP, the volume fraction of stable sI hydrate was initially approximately 40% and then increased to more than 80% in the course of the 6 hour measurement period (Figure 5e). In the long-term observation (Figure 5f), hydrates observed were mostly sI crystals, indicating that the inter-conversion almost finished within a few days, just like the case for the PVCap sample. For the PEO sample, the fraction of sI hydrate was 34% on average and did not show systematic change in the structure with time during the short-term observation (Figure 5g). The gradual increase in the sI fraction observed in the longer-time period (Figure 5h) suggests that it took more than one week for the complete structural transition.

These results suggest that the presence of PVP promotes the structural transition of metastable methane-ethane sII hydrate to stable methane-ethane sI hydrate (similar to PVCap). Conversely, PEO does not affect the inter-conversions significantly.

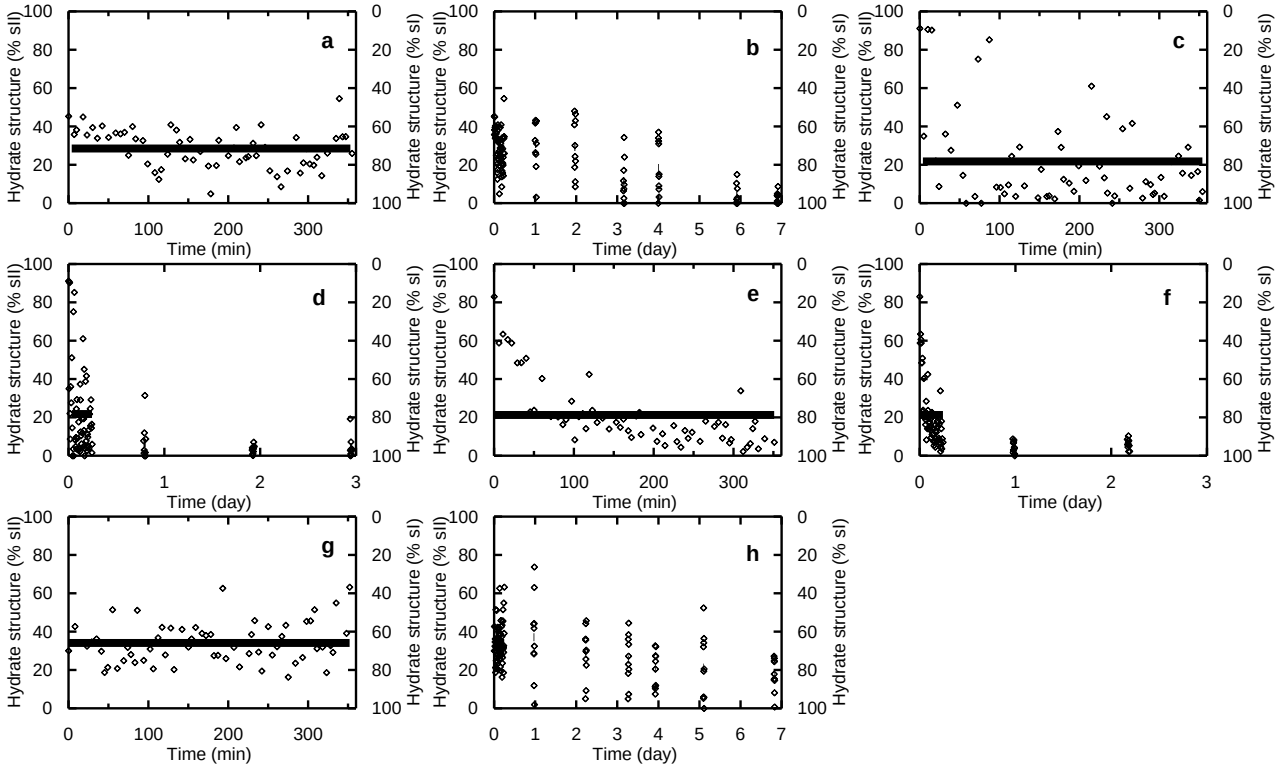

Figure 5: Methane-ethane hydrate structures at 1 ºC and 5.3 MPa of 65% CH_4 in the vicinity of the gas/hydrate interfaces vs. time after the first crystals were observed. (a) and (b) Pure system. (c) and (d) System with 0.008 wt.% PVCap. (e) and (f) System with 0.008 wt.% PVP. (g) and (h) System with 0.008 wt.% PEO. Solid symbols represent the mean values of duration of observation.

Figure 6 represents the hydrate structural compositions of the 93% CH_4 samples versus time. CSMGem predicted that sII hydrate is the stable state at these gas and pressure conditions [19]. As mentioned above, our previous results showed metastable structure I hydrate quickly converted into stable structure II hydrate in the pure system (Figure 6a). For the sample with PVCap, sI crystals survived for several days (Figure 6b and c), indicating that PVCap retards the inter-conversion at this experimental condition.

Trends in the inter-conversion for the sample with PVP were similar to those in the PVCap sample. In this system, most of the measurements showed the presence of almost pure sI hydrate throughout the short-term observation (Figure 6d). Although structure II rich crystals were found in a few measurements, the lack of observation of a systematic increase in the fraction of sII versus time indicates that considerable structural conversion did not occur in six hours. During the long-term observation, the average sII fraction increased slowly with elapsed time and attained only about 97% after four days (Figure 6e). On the other hand, metastable sI hydrate rapidly disappeared in the PEO sample (Figure 6f), just

like the case for the pure system. The initial hydrate structure was almost pure sI. However, the sII fraction rapidly increased and attainted about 100% at the end of the short-term observation.

These results suggest that the presence of PVP or PVCap inhibits the structural transition of metastable methane-ethane sI hydrate to stable methane-ethane sII hydrate significantly, while, again, PEO does not affect the inter-conversions significantly.

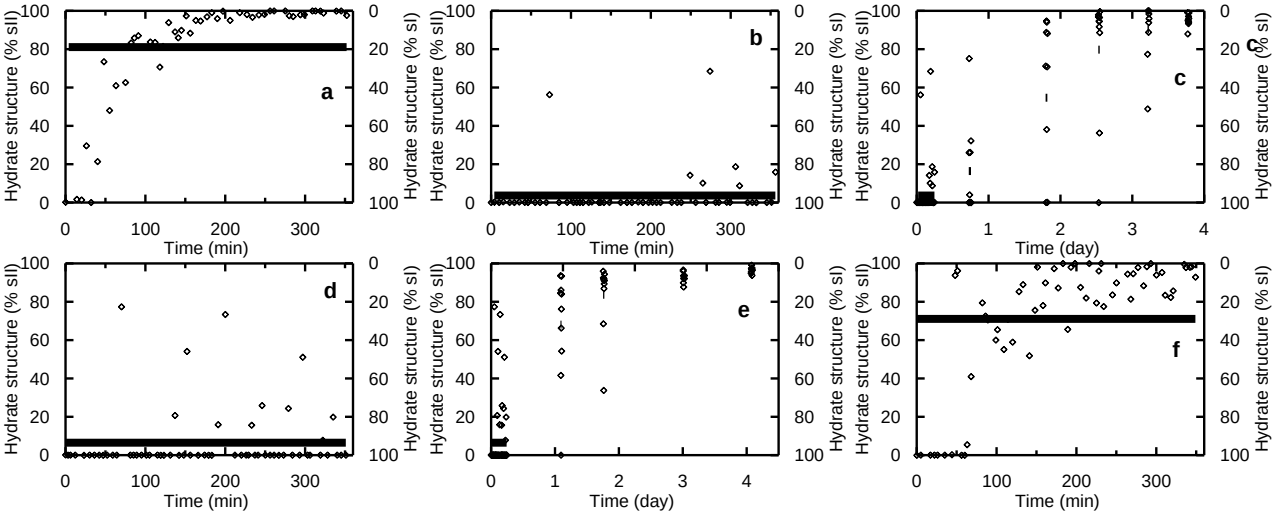

Figure 6: Methane-ethane hydrate structures at 1 ºC and 8.4 MPa of 93% CH_4 in the vicinity of the gas/hydrate interfaces vs. time after the first crystals were observed. (a) Pure system. (b) and (c) System with 0.008 wt.% PVCap (d) and (e) System with 0.008 wt.% PVP. (f) System with 0.008 wt.% PEO. Solid symbols represent the mean values of duration of observation.

DISCUSSION

Gas-composition dependence of methane-ethane hydrate metastability

In a previous study [14] we reported that the pure systems without kinetic hydrate inhibitor show the rate of structural conversion of hydrate mixtures in the 65% methane sample (Figure 5a and b) was two orders of magnitude slower than that in the 93% methane sample (Figure 6a). To explain this finding, we have proposed two possible causes: (1) the differences in the driving force and (2) kinetics of the inter-conversion.

The driving forces estimated for the two systems predict a slower conversion in the 65% CH_4 sample, which is consistent with the observations. The differences in the chemical potential of water in sI compared to sII systems calculated using CSMGem [19] are 36 J/mol for the 65% C1 sample and 66 J/mol for the 93% C1 sample. This indicates that the driving force of the hydrate structural transition in the 65% C1 sample is lower than that in the 93% C1 sample.

The kinetics of inter-conversion includes the mass transfer of guest molecules and water rearrangement for cage formation. Redistribution of guest gases in hydrate crystals is required for the structural transition, because the gas composition in sI hydrate is different from that in sII hydrate. CSMGem [19] can be used to estimate guest compositions in sI and sII crystals, i.e., (stable) sI contains 40% methane and (metastable) sII contains 66% methane for the 65% C1 gas mixture at 1 ºC, 5.3 MPa; for the 93% C1 gas mixture at 1 ºC 8.4 MPa, (metastable) sI contains 78% methane and (stable) sII contains 76% methane.

For the 65% methane gas mixture, there is a considerable difference in the guest compositions between the sI and sII hydrates, while the estimations for the two structures are about the same in the 93% methane gas mixture. This means that in the 65% methane system many more guest molecules have to redistribute when changing hydrate structure compared with the 93% methane system. This larger gas transportation may result in a slower structural transition rate.

Any water transport between sI and sII should be similar because water concentrations in sI and sII crystals are about the same. However, the crystalline water must break hydrogen bonds and rearrange to make the new cage structures during the inter-conversion of sI and sII. It seems

reasonable to suppose that the energy for breaking the hydrogen bonding of the metastable cage structure is related to the energy barrier for the water rearrangement. Previous theoretical studies calculated the hydrogen-bonding strength of water cages using the intermediate neglect of differential overlap self consistent field restricted Hartree-Fock method. These calculations showed that the average bonding strength between water molecules in $5^{12}6^4$, 7.05 kcal/mol, is stronger than those in 5^{12}, 6.67 kcal/mol, and $5^{12}6^2$, 6.69 kcal/mol [20, 21].

Because sII contains the strongly bonded cages ($5^{12}6^4$; in addition to 5^{12}) while sI consists only of the cages with weaker bonding strength (5^{12} and $5^{12}6^2$), the water rearrangement from sII is considered to require a higher activation energy compared with that from sI.

In the present study, we investigated the pure sample formed from 59% methane in ethane at 4.7MPa to clarify which factor, driving force or kinetics, is more important for determining the rate of the inter-conversion.

Since the difference in the chemical potential of water between the sI and sII systems calculated for this sample using CSMGem [19] (66 J/mol) is approximately the same as that for the 93% C1 sample, the observed difference in the conversion rate between the two samples can be considered to be solely due to the kinetic effects. Also, a considerable mass transfer effect can be expected for this sample, like the case for the 65% C1 sample: CSMGem [19] predicted that (stable) sI contains 35% methane and (metastable) sII contains 65% methane for the 59% C1 gas mixture at 1 ºC. The experimental result is that the structural transition rate in the 59% C1 system was still much slower than the observation at 93% methane: it proceeded with timescale of days (Figure 4a and b).

From the above arguments, we suggest that the kinetic processes are the main rate-determining factors of the hydrate inter-conversion.

Effect of kinetic hydrate inhibitors on the hydrate structural conversion

Analyses of hydrate structures show the presence of PVCap and PVP affects the metastability of the methane-ethane hydrates significantly, while PEO has no considerable influence on the inter-conversion (Figures 5 and 6).

It is well known that hydrate formation is significantly retarded by the addition of kinetic hydrate inhibitors [15, 22]. Larsen et al. [23] proposed that kinetic inhibitors adsorbs onto hydrate surfaces through hydrogen bonding. As a result of surface pinning by the adsorbent, crystal surfaces have micro curvatures, resulting in crystal-growth inhibition due to the Gibbs-Thomson (Kelvin) effect.

The adsorption of hydrate inhibitors to hydrate surfaces was observed using small-angle neutron scattering [24], which was also supported by molecular simulations [25, 26]. In the neutron study [24], considerable neutron scattering from polymers adsorbed to a sII THF-hydrate surface was observed in PVCap and PVP samples while the signal was not clearly detected from the system with PEO, consistent with the effectiveness of the inhibitors.

Assuming that adsorption of PVCap and PVP onto the hydrate surface occurred in our experiments, adsorbed polymers may disturb the gas capture or release and water rearrangement at crystal interfaces, these interfacial phenomena are essential for the structural conversion as discussed above. This idea can qualitatively account for the inhibition of the inter-conversion by PVCap and PVP observed in the 93% methane samples (sII). Following this line of thinking, the ineffectiveness of PEO on the hydrate conversion is probably due to its lack of ability to adsorb onto the hydrate surface.

However, the explanation of the opposite tendency of promotion of the structural transition by PVCap and PVP found in the 65% methane samples (sI) is unclear.

Although it is known that kinetic inhibitors retard both the hydrate nucleation and subsequent growth in most cases [15, 22], results of gas consumption measurements on carbon dioxide hydrate formation [27] suggested that PVP delays the nucleation but promotes crystal growth. More recently Lee and Englezos [28] found from visual observation of methane-ethane hydrate formation that when inhibitors GHI 101 were present, the nucleation inhibition was followed by catastrophic crystal growth.

The above diverse actions of kinetic inhibitors imply the existence of complicated interactions between polymers, water and gas molecules at crystal surfaces which may depend on hydrate structure and guest composition.

To clarify the mechanism of interactions between polymers, water and guest molecules at the hydrate surface, *in situ* observation of the hydrate surface phenomena, for example using small-angle

neutron scattering [24, 29], may be required. Understanding the probable difference in the structure of adsorbed polymers and crystal interfaces between the inhibited and promoted systems will provide important clues to clarify the fundamental mechanism of kinetic hydrate inhibition.

CONCLUSIONS

In order to understand methane-ethane hydrate metastability, structures of hydrates formed from liquid water and methane-ethane gas mixtures have been measured as a function of time after the first hydrate crystals were observed using Raman spectroscopy. To investigate the effect of gas composition and the presence of kinetic hydrate inhibitors on the phenomenon, three methane-ethane gas mixtures of 59, 65 or 93% CH_4 and water, with and without inhibitors (0.008 wt.% PVP or PEO) have been studied.

Initially, mixtures of sI and sII formed in all experiments, and the subsequent conversion from metastable to stable structures was observed. It was found that the degree of metastability depends on gas composition. When the results of the pure systems are compared, at 59% CH_4 the two structures coexisted for several days, while at 93% CH_4 Raman signals from sI (metastable) quickly weakened and disappeared in a few hours, indicating that the structural conversion is much slower at the lower concentration of CH_4.

This discrepancy can be explained as the difference in the kinetics of the inter-conversion, namely, the degree of guest-gas redistribution and activation energy for water rearrangement. Also, it was found that the presence of PVP or PVCap affects the metastability. At 65% CH_4 the inhibited system had less metastable sII than the pure system, while at 93% CH_4 the conversion rate was two orders of magnitude slower than the pure system. In contrast, PEO did not significantly influence the hydrate metastability.

These findings have important implications in pipeline flow assurance, and in crystal growth processes in general.

ACKNOWLEDGEMENT

The present study is supported by the ACS Petroleum Research Fund (# 42254-AC2).

REFERENCES

[1] Sloan ED, Koh CA. *Clathrate Hydrates of Natural Gases*, 3rd ed.; CRC Press - Taylor and Francis, Boca Raton, Fla, 2008.

[2] Sloan, ED. *Gas hydrates: Review of physical/chemical properties*. Energy Fuels 1998; 12(2): 191-196.

[3] Koh CA. *Towards a fundamental understanding of natural gas hydrates*. Chem. Soc. Rev. 2002; 31(3): 157-167.

[4] Sloan ED. *Fundamental principles and applications of natural gas hydrates*. Nature 2003; *426*: 353-363.

[5] Koh CA., Sloan ED. *Natural gas hydrates: Recent advances and challenges in energy and environmental applications*. AlChE J. 2007; 53(7): 1636-1643.

[6] Ballard AL, Sloan ED. *Structural transitions in methane+ethane gas hydrates — Part II: modeling beyond incipient conditions*. Chem. Eng. Sci. 2000; 55(23): 5773-5782.

[7] Hendriks EM, Edmonds B, Moorwood RAS, Szczepanski R. Hydrate structure stability in simple and mixed hydrates. Fluid Phase Equilib. 1996; 117(1-2): 193-200.

[8] Subramanian S, Kini RA, Dec SF, Sloan ED. *Evidence of structure II hydrate formation from methane+ethane mixtures*. Chem. Eng. Sci. 2000; 55(11): 1981-1999.

[9] Subramanian S, Ballard AL, Kini RA, Dec SF, Sloan ED. *Structural transitions in methane+ethane gas hydrates — Part I: upper transition point and applications*. Chem. Eng. Sci. 2000; 55(23): 5763-5771.

[10] Ripmeester JA. *Hydrate research-from correlations to a knowledge-based discipline: the importance of structure*. Ann. NY Acad Sci. 2000; 912: 1-16.

[11] Hester K, Sloan ED. *sII structural transitions from binary mixtures of simple sI formers*. Int. J. Thermophys. 2005; 26(1): 95-106.

[12] Takeya S, Kamata Y, Uchida T, Nagao J, Ebinuma T, Narita H, Hori A, Hondoh T. *Coexistence of structure I and II hydrates formed from a mixture of methane and ethane gases*. Can. J. Phys. 2003; 81: 479-484.

[13] Bowler KE, Stadterman LL, Dec SF, Koh CA, Sloan ED, Creek JL. *NMR studies of binary gas hydrates decomposition*. Proc. 5th Int. Conf. Gas Hydrates 2005; 5: 5030.

[14] Ohno H, Strobel TA, Dec SF, Sloan ED, Koh CA. Raman studies of methane-ethane hydrate metastability. J. Phys. Chem. A 2008, under review.

[15] Lederhos JP, Long JP, Sum A, Christiansen RL, Sloan ED. *Effective kinetic inhibitors for natural gas hydrates*. Chem. Eng. Sci. 1996; 51(8): 1221-1229.
[16] Subramanian S. *Measurements of Clathrate Hydrates Containing Methane and Ethane Using Raman Spectroscopy*. Ph.D. Thesis, Colorado School of Mines, 2000.
[17] Hester KC. *Probing Hydrate Stability and Structural Characterization of Both Natural and Synthetic Clathrate Hydrates*. Ph.D. Thesis, Colorado School of Mines, 2007.
[18] Uchida T, Takeya S, Kamata Y, Ikeda IY, Nagao J, Ebinuma T, Narita H, Zatsepina O, Buffett BA. *Spectroscopic Observations and Thermodynamic Calculations on Clathrate Hydrates of Mixed Gas Containing Methane and Ethane: Determination of Structure, Composition and Cage Occupancy*. J. Phys. Chem. B 2002; 106(48): 12426-12431.
[19] Ballard AL, Sloan ED. *The next generation of hydrate prediction I. Hydrate standard states and incorporation of spectroscopy*. Fluid Phase Equilib. 2002; 194-197: 371-383.
[20] Khan A. *Theoretical studies of tetrakaidecahedral structures of $(H_2O)_{24}$, $(H_2O)_{25}$ and $(H_2O)_{26}$ clusters*. Chem. Phys. Lett. 1996; 253(3-4): 299-304.
[21] Khan A. *Theoretical studies of large water clusters: $(H_2O)_{28}$, $(H_2O)_{29}$, $(H_2O)_{30}$, and $(H_2O)_{31}$ hexakaidecahedral structures*. J. Chem. Phys. 1997; 106(13): 5537-5540.
[22] Kelland MA. *History of the development of low dosage hudrtae inhibitors*. Energy Fuels 2006; 20(3): 825-847.
[23] Larsen R, Knight CA, Sloan ED. *Clathrate hydrate growth and inhibition*. Fluid Phase Equilib. 1998; 150-151: 353-360.
[24] King HE, Hutter JL, Lin MY, Sun T. *Polymer conformations of gas-hydrate kinetic inhibitors: A small-angle neutron scattering study*. J. Chem. Phys. 2000; 112(5): 2523-2532.
[25] Carver TJ, Drew MGB, Rodger PM. *Inhibition of crystal-growth in methane hydrate*. J. Chem. Soc., Faraday Trans. 1995; 91(19): 3449-3460.
[26] Anderson BJ, Tester JW, Borghi GP, Trout BL. *Properties of inhibitors of methane hydrate formation via molecular dynamics simulations*. J. Am. Chem. Soc. 2005; 127(50): 17852-17862.
[27] Motie RE. Ph.D. Thesis, King's College London, 1998.
[28] Lee JD, Englezos P. *Unusual kinetic inhibitor effects on gas hydrate formation*. Chem. Eng. Sci. 2006; 61(5): 1368-1376.
[29] Hutter JL, King HE, Lin MY. *Polymeric Hydrate-Inhibitor Adsorption Measured by Neutron Scattering*. Macromolecules 2000; 33(7): 2670-2679.